Supporting Information: Differentiating the Mechanism of Self-Assembly in Supramolecular Polymers through Computation

Divya B. Korlepara,[†] Will R. Henderson,[‡] Ronald K. Castellano,[‡] and Sundaram Balasubramanian[*,†]

Chemistry and Physics of Materials Unit, Jawaharlal Nehru Centre for Advanced Scientific Research, Bangalore 560 064, India, and Department of Chemistry, University of Florida, P.O. Box 117200, Gainesville, FL 32611 (USA)

E-mail: bala@jncasr.ac.in;castellano@chem.ufl.edu

Phone: +91 80 2208 2767. Fax: +91 80 2208 2766

---

[*]To whom correspondence should be addressed

[†]Chemistry and Physics of Materials Unit, Jawaharlal Nehru Centre for Advanced Scientific Research, Bangalore 560 064, India

[‡]Department of Chemistry, University of Florida, P.O. Box 117200, Gainesville, FL 32611 (USA)

Computational Details

Gas-Phase calculations

Quantum Chemical Calculations:

Structures of the molecules were optimized using density functional theory (DFT) using the Quickstep method (QS) in CP2K software.[1] The molecules were placed in a cubic box of edge dimension 200 Å. The Perdew-Burke-Ernzerhof (PBE) functional [2] with double ζ single polarization basis set and an energy cutoff of 280Ry was used. The Goedecker-Tetter-Hutter (GTH)[3] pseudopotentials described the interaction of the valence electrons with the nuclei and core electrons. Empirical DFT-D3[4] corrections were used to include the van der Waals interactions.

Charge Calculations:

The partial charges on the atoms of all the molecules used in force-field calculations are calculated from the quantum optimized structures (for both [2.2]pCpTA and BTA) whose electron density cube files were analyzed using the Density Derived Electrostatic and Chemical method (DDEC/c3)[5,6] to obtain the site charges which were used in force field based MD simulations.

Molecular modelling in MD simulations:

The atoms of [2.2]pCpTA-met (S_p), [2.2]pCpTA-hex (S_p), BTA-met (2:1) and BTA-hex (2:1) were modeled through an all-atom model. DREIDING force field[7] was used for parameterization of bonded and non-bonded interactions. [2.2]pCpTA-hex molecule is soluble in chloroform.[8] Chloroform was modeled in all-atom representation and the parameters were taken from the DREIDING force field.[7] The interaction parameters are provided in Tables S1- S5 for the sake of completeness. The atom notations are: C_3-sp^3, C_2-carbon atom of amide group, C_R-aromatic carbon, H-Hydrogen, H_{hb}-Hydrogen participating in hydrogen bond,

N_R-Nitrogen, O_2-Oxygen and Cl-Chlorine of chloroform

$$E = \sum^{\text{bond}} K_r(r - r_o)^2 + \sum^{\text{angle}} K_\theta(\theta - \theta_0)^2 + \sum^{\text{dihedral}} K_\phi[1 + dcos(n\phi)]$$
$$+ \sum^{\text{improper}} (1/2)K_\phi \left[\frac{1 + cos(\omega_0)}{sin(\omega_0)}\right]^2 [cos(\omega) - cos(\omega_0)] + E_{nb} \tag{1}$$

$$E_{nb} = E_{vdW} + E_Q + E_{hb}$$

where, $\quad E_{vdW} = Aexp(-Cr_{ij}) - \dfrac{B}{r_{ij}^6} \quad$ for [2.2]pCpTA-hex and [2.2]pCpTA-met molecule

For chloroform molecule, $\quad E_{vdW} = \begin{cases} C(r) & r < r_{in} \\ S(r) * LJ(r) & r_{in} < r < r_{out} \\ 0 & r > r_{out} \end{cases}$

$$\text{Where,} \quad LJ(r) = 4\epsilon[\left(\frac{\sigma}{r}\right)^{12} - \left(\frac{\sigma}{r}\right)^6]$$

$$S(r) = \frac{[r_{out}^2 - r^2]^2[r_{out}^2 + 2r^2 - 3r_{in}^2]}{[r_{out}^2 - r_{in}^2]^3}$$

$$E_Q = C(r) = \frac{q_i q_j}{4\pi\varepsilon_0 r_{ij}}$$

$$E_{hb} = D_{hb}[5\left(\frac{R_{hb}}{R_{DA}}\right)^{12} - 6\left(\frac{R_{hb}}{R_{DA}}\right)^{10}]cos^4(\theta_{DHA})$$

$$\tag{2}$$

3

Force-field parameters

Table S1: Non-bonded interaction parameters of atoms in [2.2]pCpTA-met and [2.2]pCpTA-hex and of those in chloroform molecule.

Atom pairs	pair style	A (kcal/mole)	C ($\mathring{A}^{-1}$)	B (($\mathring{A}^6$*kcal)/mole)
C_2,C_2	$E_{vdW}([2.2]pCpTA)$	88366.7126395	0.2777754	583.0176588
C_2,C_3	$E_{vdW}([2.2]pCpTA)$	88366.7126395	0.2777754	583.0176588
C_2,C_R	$E_{vdW}([2.2]pCpTA)$	88366.7126395	0.2777754	583.0176588
C_2,H	$E_{vdW}([2.2]pCpTA)$	17353.2373205	0.2675420	135.2359749
C_2,H_{hb}	$E_{vdW}([2.2]pCpTA)$	1199.2541785	0.2718906	11.1370044
C_2,N_R	$E_{vdW}([2.2]pCpTA)$	73336.2339858	0.2709990	438.3045053
C_2,O_R	$E_{vdW}([2.2]pCpTA)$	69732.3531147	0.2645411	395.6858342
C_2,Cl	$E_{vdW}([2.2]pCpTA)$	141410.6995235	0.2813384	1051.9927862
C_3,C_3	$E_{vdW}([2.2]pCpTA)$	88366.7126395	0.2777754	583.0176588
C_3,C_R	$E_{vdW}([2.2]pCpTA)$	88366.7126395	0.2777754	583.0176588
C_3,H	$E_{vdW}([2.2]pCpTA)$	17353.2373205	0.2675420	135.2359749
C_3,H_{hb}	$E_{vdW}([2.2]pCpTA)$	1199.2541785	0.2718906	11.1370044
C_3,N_R	$E_{vdW}([2.2]pCpTA)$	73336.2339858	0.2709990	438.3045053
C_3,O_R	$E_{vdW}([2.2]pCpTA)$	69732.3531147	0.2645411	395.6858342
C_3,Cl	$E_{vdW}([2.2]pCpTA)$	141410.6995235	0.2813384	1051.9927862
C_R,C_R	$E_{vdW}([2.2]pCpTA)$	88366.7126395	0.2777754	583.0176588
C_R,H	$E_{vdW}([2.2]pCpTA)$	17353.2373205	0.2675420	135.2359749
C_R,H_{hb}	$E_{vdW}([2.2]pCpTA)$	1199.2541785	0.2718906	11.1370044
C_R,N_R	$E_{vdW}([2.2]pCpTA)$	73336.2339858	0.2709990	438.3045053
C_R,O_R	$E_{vdW}([2.2]pCpTA)$	69732.3531147	0.2645411	395.6858342
C_R,Cl	$E_{vdW}([2.2]pCpTA)$	141410.6995235	0.2813384	1051.9927862
H,H	$E_{vdW}([2.2]pCpTA)$	3407.7859921	0.2580359	31.3691509
H,H_{hb}	$E_{vdW}([2.2]pCpTA)$	235.5065810	0.2620786	2.5833242
H,N_R	$E_{vdW}([2.2]pCpTA)$	14401.5889528	0.2612501	101.6685107
H,O_R	$E_{vdW}([2.2]pCpTA)$	13693.8677062	0.2552434	91.7827423
H,Cl	$E_{vdW}([2.2]pCpTA)$	141410.6995235	0.2813384	1051.9927862
H_{hb},H_{hb}	$E_{vdW}([2.2]pCpTA)$	16.2754791	0.2662500	0.2127429
H_{hb},N_R	$E_{vdW}([2.2]pCpTA)$	995.2705314	0.2653949	8.3726438
H_{hb},O_R	$E_{vdW}([2.2]pCpTA)$	946.3610601	0.2591984	7.5585273
H_{hb},Cl	$E_{vdW}([2.2]pCpTA)$	1919.1318453	0.2753033	20.0955291
N_R,N_R	$E_{vdW}([2.2]pCpTA)$	60862.3208284	0.2645453	329.5111845
N_R,O_R	$E_{vdW}([2.2]pCpTA)$	57871.4315792	0.2583879	297.4710649
N_R,Cl	$E_{vdW}([2.2]pCpTA)$	117357.8583902	0.2743891	790.8734337
O_R,O_R	$E_{vdW}([2.2]pCpTA)$	55027.5202694	0.2525106	268.5463760
O_R,Cl	$E_{vdW}([2.2]pCpTA)$	111590.6718585	0.2677707	713.9726163
Cl,Cl	$E_{vdW}(CHCl3)$	226295.4606144	0.2849939	1898.2080654

Table S2: Bond parameters

Bonded Atoms list	K_r (kcal/mol/Å^2)	r_0 (Å)
C_2,C_R	525	1.39
C_2,N_R	525	1.34
C_2,O_2	525	1.35
C_3,C_3	350	1.53
C_3,C_R	350	1.46
C_3,H	350	1.09
C_3,N_R	350	1.41
C_R,C_R	525	1.39
C_R,H	350	1.02
H_{hb},N_R	350	0.97
C_3,Cl	350	1.757

Table S3: Angle parameters

Atoms forming angles	K_θ (kcal/mol/rad^2)	θ_0 (°)
C_3,C_3,C_3	50	109.47
C_3,C_3,C_R	50	109.47
C_3,C_3,H	50	109.47
C_3,C_3,N_R	50	109.47
C_3,C_R,C_R	50	120.0
C_3,N_R,C_R	50	120.0
C_3,N_R,H_{hb}	50	120.0
C_R,C_3,H	50	109.47
C_R,C_R,C_R	50	120.0
C_R,C_R,C_2	50	120.0
C_R,C_R,H	50	120.0
C_R,C_2,N_R	50	120.0
C_R,C_2,O_R	50	120.0
C_2,N_R,H_{hb}	50	120.0
H,C_3,H	50	109.47
H,C_3,N_R	50	109.47
N_R,C_2,O_R	50	120.0
Cl,C_3,Cl	50	109.471
Cl,C,H	50	109.471

Table S4: Dihedral parameters

Atoms List (order specific)	K_ϕ (kcal/mol)	d	n
C_3,C_3,C_3,C_3	0.111	1	3
$C_3,C_3,C_3,$H	0.111	1	3
C_3,C_3,C_3,N_R	0.111	1	3
C_3,C_3,C_R,C_R	0.083	-1	6
C_3,C_3,N_R,C_2	0.083	-1	6
C_3,C_3,N_R,H_{hb}	0.083	-1	6
C_3,C_R,C_R,C_R	3.125	-1	2
C_3,C_R,C_R,C_2	3.125	-1	2
$C_3,C_R,C_R,$H	3.125	-1	2
C_R,C_3,C_3,C_R	0.111	1	3
$C_R,C_3,C_3,$H	0.111	1	3
C_R,C_R,C_R,C_R	3.125	-1	2
C_R,C_R,C_R,C_2	3.125	-1	2
$C_R,C_R,C_R,$H	3.125	-1	2
C_R,C_R,C_2,N_R	3.125	-1	2
C_R,C_R,C_2,O_R	3.125	-1	2
C_R,C_2,N_R,C_3	3.125	-1	2
C_R,C_2,N_R,H_{hb}	3.125	-1	2
$C_2,C_R,C_R,$H	3.125	-1	2
H,$C_3,C_3,$H	0.111	1	3
H,C_3,C_3,N_R	0.111	1	3
H,C_3,N_R,C_R	0.083	-1	6
H,C_3,N_R,C_2	0.083	-1	6
H,C_3,N_R,H_{hb}	0.083	-1	6
O_R,C_2,N_R,C_3	3.125	-1	2
O_R,C_2,N_R,H_{hb}	3.125	-1	2

Table S5: Improper dihedral parameters

Atoms List (order specific)	K_ϕ (kcal/mol)	ω_0 (°)
C_3,C_2,N_R,H_{hb}	40	0
C_R,C_R,C_R,C_2	40	0
$C_R,C_R,C_R,$H	40	0
C_R,N_R,C_2,O_R	40	0

Force-field based calculations:

To obtain the energy differences between conformers within the force field, gas phase geometry optimizations using the force field were carried out on structures [2.2]pCpTA-met and BTA-met oligomers obtained from quantum chemical calculations. These were carried out in LAMMPS[9] code. The dimensions of the simulation box (cubic) was taken to be 200 Å.

Bulk simulations:

MD simulations to determine the self diffusion coefficient of [2.2]pCpTA-hex in chloroform:

Three independent simulations were performed to calculate the self diffusion coefficient of [2.2]pCpTA-hex in chloroform. Each system has 5 [2.2]pCpTA-hex molecules dispersed in chloroform (69613 molecules) in a cubic box of edge dimensions 212 Å. The simulations were performed at 298.15 K, the positions and velocities were updated at every 0.5 fs using velocity-Verlet integrator. The system was equilibrated under NVT ensemble for 10 ns followed by the trajectory in the NPT ensemble. Coordinates were saved every 1 fs.

MD simulations of preformed decamer ([2.2]pCpTA-hex) in chloroform:

A preformed 10-mer was soaked in a cubic box of size 100 Å filled with 7520 chloroform molecules. The system was equilibrated for 10 ns in the canonical ensemble using Nosé-Hoover thermostat[10,11] with a damping constant of 1000 ps, and the position and velocities were updated using the velocity-Verlet algorithm[12] every 0.5 fs. Atom positions were saved every 1.25 ps.

Free energy Simulations:

Method: Adaptive biasing force method (ABF)

The adaptive biasing force (ABF)[13] method, based on the thermodynamic integration (TI) scheme to estimate the free energy profiles was used to study the dissociation free energies of oligomers in solution. The free energy (A_ξ) is estimated as a function of a collective variable (ξ), which is calculated from the average of a force F_ξ exerted on ξ.

$$A(\xi) = -\beta^{-1} \ln P(\xi) + A_0 \tag{3}$$

$$\nabla_\xi A(\xi) = \langle -F_\xi \rangle_\xi \tag{4}$$

Simulation Setup for [2.2]pCpTA-hex in chloroform:

We performed free energy calculations using the Adaptive Biasing Force (ABF)[13] method for the formation of oligomers of various sizes of [2.2]pCpTA-hex in chloroform present in a cubic box of size 100 Å. The systems were prepared by inserting a preformed oligomer in such a way that stacks aligned along the z-axis in a simulation box which contains 7520 chloroform molecules. The reaction coordinate (ξ) is chosen to be the distance along the stacking direction between the Nth molecule (tip of the oligomer) and $(N-1)^{th}$ molecule of an oligomer size N. The same was implemented in the colvars module[14] of LAMMPS package as "distanceZ". It is worth noting that the molecule taken away from the tip of the oligomer can interact with the stack from the lateral side by its unrestricted motion throughout the simulation box. To avoid such interactions, we restricted the motion of the molecule seperated from the stack in XY-plane by constructing a cylinder of radius 5 Å which can be included by the "distanceXY"[14] keyword.

The upper bound of the reaction coordinate is taken in such a way that the Nth and $(N-1)^{th}$ molecules do not interact with each other (22.0 Å) whereas the lower bound is considered

as the center of mass-center of mass distance (6.0 Å) between them.

Simulation Setup for BTA-hex in *n*-nonane:

The preformed BTA-hex oligomers were solvated in a cubic box which contained *n*-nonane. The free energy calculations were preformed using the distanceZ & distanceXY[14] keyword in LAMMPS package, as discussed in the previous section. As the π-π distance in the BTA-hex oligomers is about 3.5 Å from our earlier reports,[15,16] we consider the lower bound of the reaction coordinate to be less than the π-π distance & is taken to be 2.5 Å and the upper boundary is taken as 19 Å. The system details are given in Table S6.

Table S6: System sizes of BTA-hex in *n*-nonane for ABF simulations.

Range of oligomer size	Number of *n*-nonane molecules	Length of cubic box (Å)
2-5	215	40.00
6-10	1720	80.00

The details of the ABF calculations are given in Table S7. ABF simulations were performed under NVT ensemble at ambient conditions. Atom position and velocities are updated every 0.5 fs using velocity-Verlet algorithm. The coordinates of the atoms were saved every 2.5 ps. Each window is simulated for 25 ns.

Table S7: Windows setup in free-energy calculations performed using the ABF method

| Solute	Units	Bin width	Window 0	Window 1	Window 2	Window 3	Window 4	Window 5
[2.2]pCpTA-hex in chloroform	Å	0.1	[6.0,6.5]	[6.5,10.0]	[10.0,13.0]	[13.0,16.0]	[16.0,19.0]	[19.0,22.0]
BTA-hex in *n*-nonane	Å	0.1	[3.0,6.0]	[6.0,10.0]	[10.0,13.0]	[13.0,16.0]	[16.0,19.0]	-

Method: Well-Tempered metadynamics (WTM)

Free energy surfaces arising due to conformational changes can be well sampled through the well-tempered metadynamics (WTM) simulations, due to its self-guiding nature. Gaussian hills are deposited along the trajectory of the collective variables. In WTM, the Gaussian hills height decrease with time. The effective Gaussian height is calculated by rescaling as

$w = \omega e^{\frac{-V(s,t)}{\Delta T}} T_G$, where V(s,t) is the history dependent potential, T_G is the time interval at which Gaussian are deposited. The free-energy surface is estimated as $\tilde{F}$(s,t)$=-(T + \Delta T) \ln(1 + \frac{\omega N(s,t)}{\Delta T})$,[17] where N(s,t) is the histogram of the collective variable 's' over the simulation time t. The simulations were performed by including PLUMED[18] to LAMMPS[9] software.

Simulation setup for WTM

One molecule of [2.2]pCpTA-hex is soaked in chloroform and is well equilibrated at ambient conditions, and later the configuration is taken for free-energy calculations. The dihedral angles (Φ & Ψ) shown in Fig. S14(a) are taken as collective variables to explore the free-energy surface (FES) which connects the anti and syn configuration of the [2.2]pCpTA-hex molecule. The simulations were performed in the NVT ensemble at 298.15 K for 400 ns & the position were updated for every 0.5 fs using the velocity-Verlet algorithm.

Structure of the molecules:
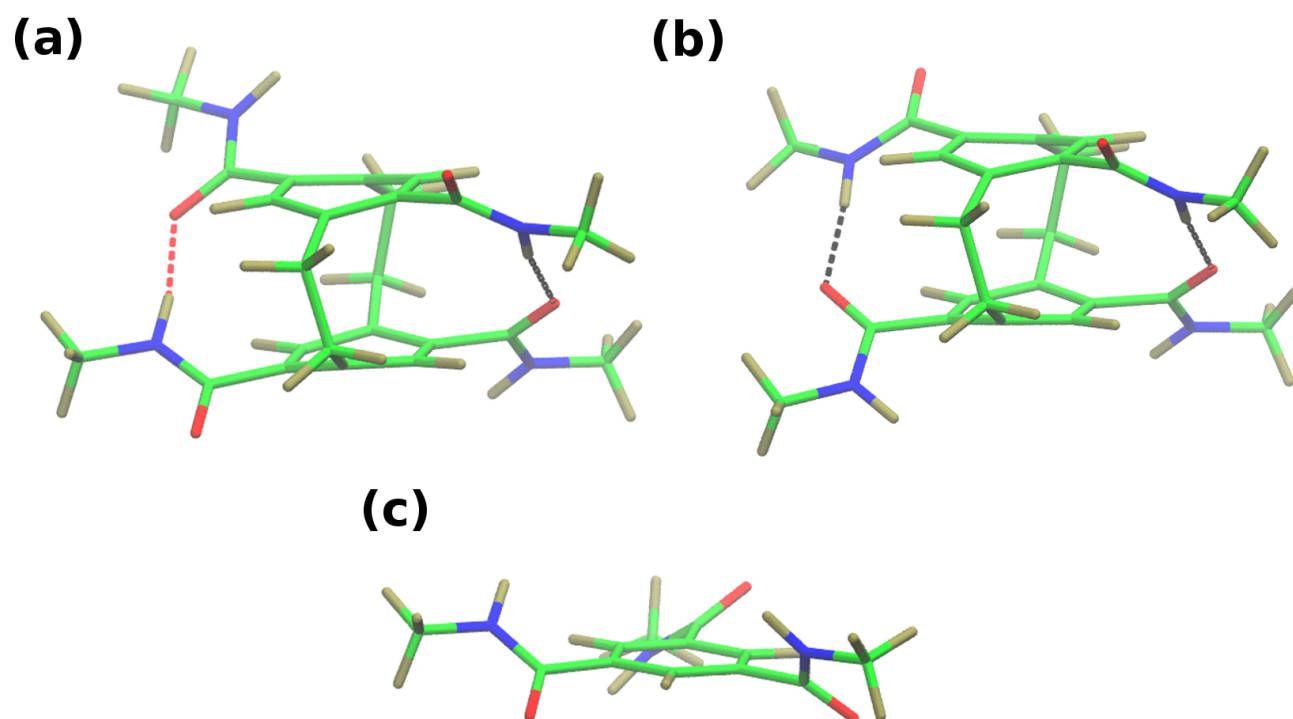
Figure S1: Structures of [2.2]pCpTA-met and BTA-met molecules. (a) anti conformer of [2.2]pCpTA-met (b) syn conformer of [2.2]pCpTA-met and (c) 2:1 conformer of BTA-met. Color scheme: Green-Carbon, Red-Oxygen, Blue-Nitrogen, Tan-Hydrogen and dashed lines represent hydrogen bonds. The hydrogen bonds are colored in red and black depending on their dipole directions.
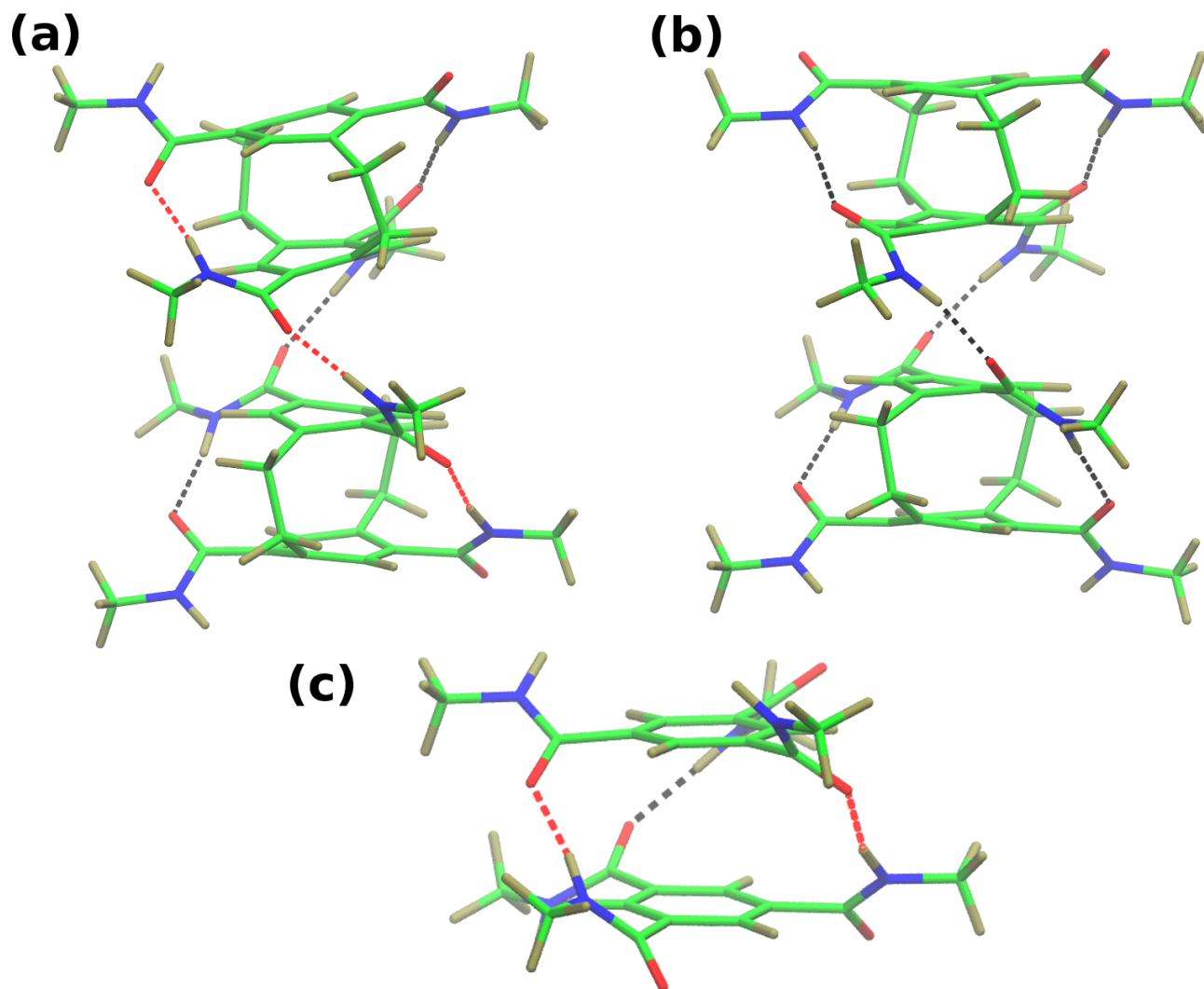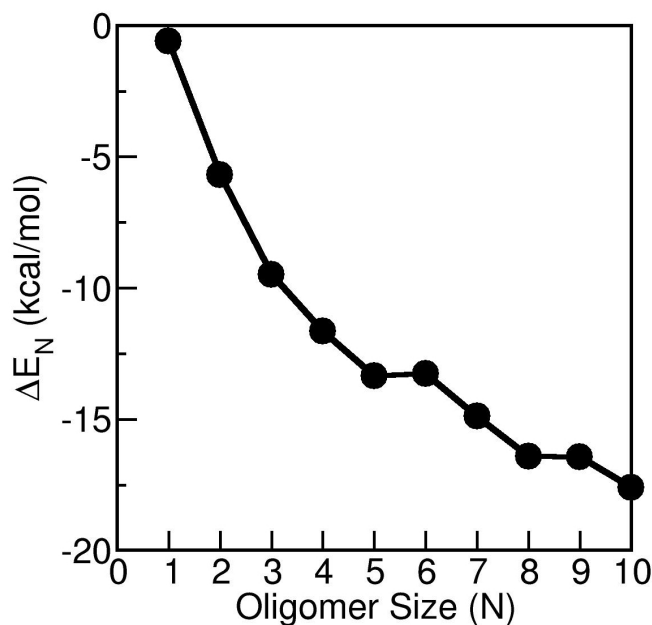
Figure S2: Dimer structures of [2.2]pCpTA-met and BTA-met molecules. (a) constructed out of anti conformers of [2.2]pCpTA-met (b) constructed out of syn conformers of [2.2]pCpTA-met and (c) 2:1 of BTA-met. See Figure S1 for the color scheme.

Results & Discussion
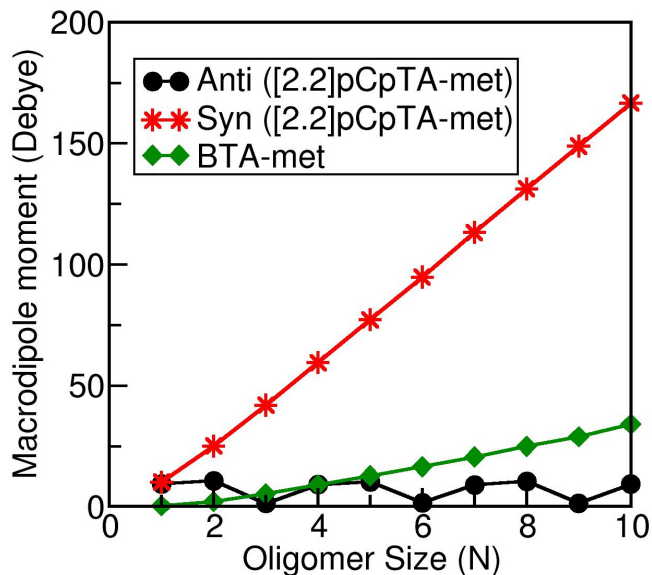
Figure S3: Evolution of total electric dipole moment of [2.2]pCpTA-met oligomers in anti & syn conformations and of oligomers of BTA-met in their 2:1 conformation. The structures were optimized using PBE-D3 level of theory in gas phase. Structures of dimer of these two molecules are shown in Fig. S2

Figure S4: Energy difference (ΔE_N) of oligomers of anti and syn conformations of [2.2]pCpTA-met. The structures were optimized using density functional theory at PBE-D3 level of theory. $\Delta E_N = E_{anti} - E_{syn}$

13

Table S8: Mean values of intermolecular π-π distances (distance between centroids of closest phenyl rings of adjacent molecules in a stack) (in Å) and intermolecular hydrogen bond (N - - - O) distance (in Å) in oligomers of [2.2]pCpTA-met and BTA-met obtained from gas phase DFT calculations. [a]

Oligomer Size (N)	π-π Distance (Å)		Hydrogen bond distance (Å)	
	Anti conformer of -met [2.2]pCpTA	2:1 conformer of BTA-met	Anti conformer of -met [2.2]pCpTA	2:1 conformer of BTA-met
2	3.72	3.52	2.78	2.96
3	3.74	3.50	2.78	2.88
4	3.79	3.41	2.79	2.87
5	3.80	3.43	2.79	2.85
6	3.85	3.40	2.79	2.85
7	3.88	3.39	2.81	2.88
8	3.87	3.39	2.81	2.78
9	3.90	3.39	2.78	2.85
10	3.89	3.38	2.78	2.89

[a] Intermolecular π-π distances reported from experiments are 3.8 Å and 3.4 Å in [2.2]pCpTA crystal[8] and BTA in liquid crystalline phase[19] respectively. The hydrogen bond distance in the case of [2.2]pCpTA with propyl tail from its experimentally determined crystal structure[8] is 2.81 Å.
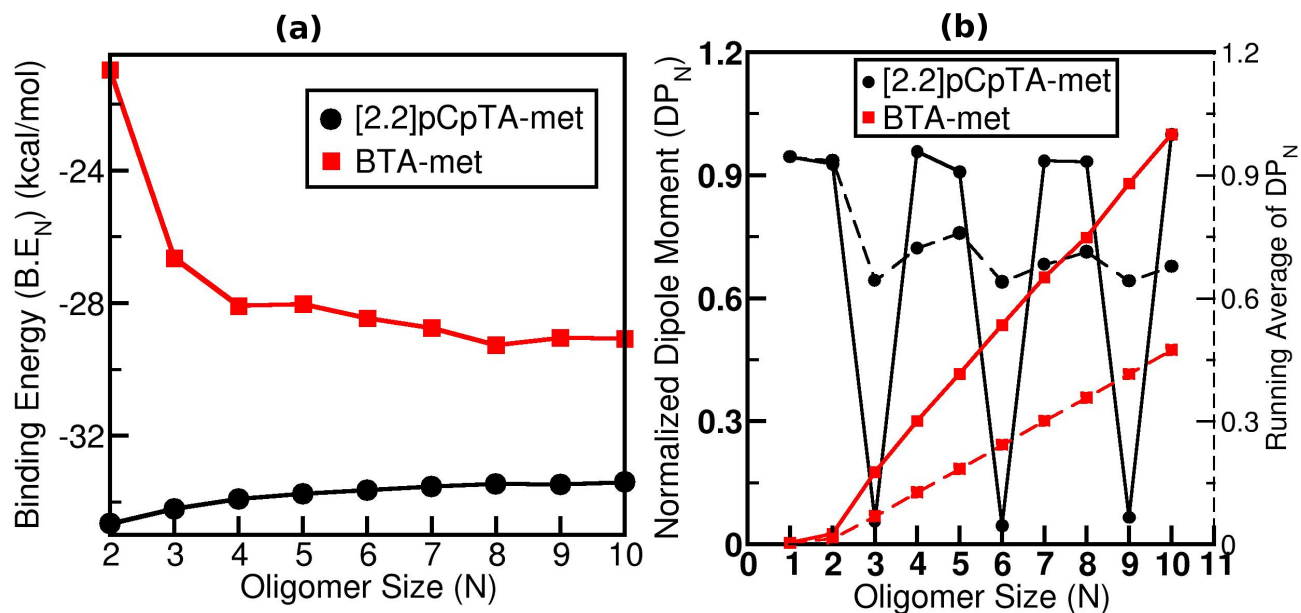
Figure S5: Results for oligomers of [2.2]pCpTA-met and BTA-met optimized using force field in gas phase. **(a)** Binding energy as a function of oligomer size,[20] **(a)** Normalized macrodipole moment (DP_N)[21] of the stack along the stacking direction and its running average.

Table S9: Mean values of Intermolecular π-π distance of oligomers of [2.2]pCpTA-met optimized using force field in gas phase.

Length of Oligomer (N)	Anti	Syn
	π-π **Distance (Å)**	
2	3.33	3.31
3	3.33	3.31
4	3.32	3.31
5	3.33	3.31
6	3.33	3.32
7	3.33	3.31
8	3.33	3.32
9	3.34	3.31
10	3.34	3.31

Table S10: Electric dipole moment of oligomers of [2.2]pCpTA-met optimized using force field in gas phase.

Oligomer Size (N)	Anti	Syn
	Dipole moment (Debye)	
1	13.05	7.76
2	12.15	17.51
3	0.883	27.80
4	13.15	37.70
5	11.83	48.41
6	5.87	57.91
7	16.46	68.88
8	12.62	78.85
9	15.57	88.75
10	21.04	99.22

A preformed stack containing ten molecules was equilibrated for 10 ns in the canonical ensemble. Intermolecular distances and twist angles (see Fig. S6) between successive molecules in a stack were calculated from the last 5 ns of the trajectory. The simulations showed the stack to be stable with intact intermolecular hydrogen bonds and the equilibrated structure exhibited a mean intermolecular distance of 6.4 Å and a mean twist angle of 118°; their distributions are shown in Fig. S7(a). The twist angle is defined in Fig. S6. (Fig. S5 compares the binding energy and normalized dipole moments along the stacking direction obtained from gas phase, force field based calculations against the results obtained from gas phase quantum chemical calculations).
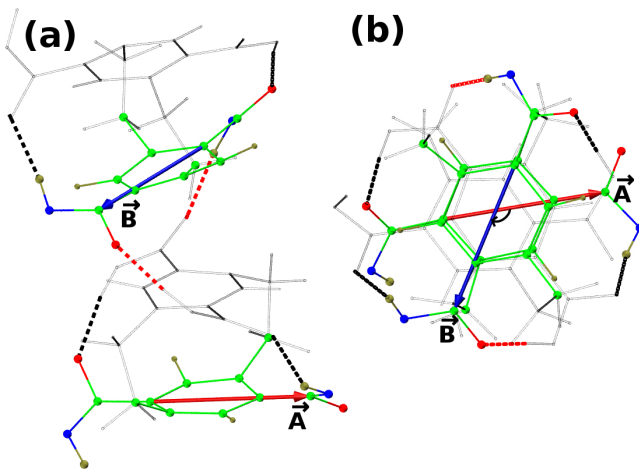
Figure S6: Twist angle between successive molecules in a stack **(a)** Side view **(b)** Top view. The color scheme: Green-Carbon, Red-Oxygen, Blue-Nitrogen, Tan-Hydrogen and dotted lines represents the hydrogen bonds (Red-Inter, Black-Intra) and the angle between $\vec{A}$ and $\vec{B}$ is defined as twist angle. Alkyl tails are not shown for clarity.

In recent times, the interaction between a halogen atom and nucleophile has gained much attention[22,23] due to its comparable strength to hydrogen bonding.[24,25] The distribution of chlorine atom from the solvent (here, chloroform) to the oxygen of the amide group (in a preformed stack of [2.2]pCpTA-hex) is studied through the radial distribution function (RDF) shown in Fig. S7(b). The non-negligible first peak in the RDF signifies reasonable ordering of the solvent chloroform molecules around the stack. The mean number of chlorine atoms within a distance of 4 Å from the amide oxygen was found to be 0.7 (see the running
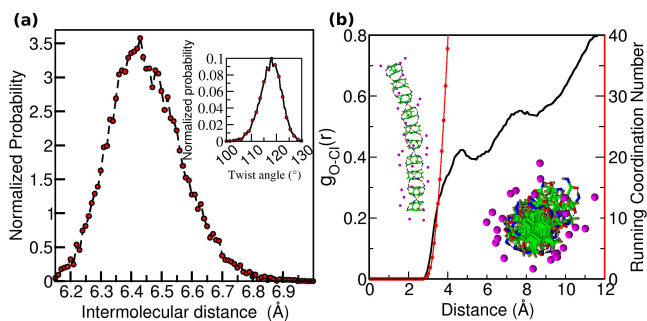
Figure S7: Structural properties of a preformed decamer of [2.2]pCpTA-hex in chloroform solvent at ambient conditions: **(a)** Intermolecular distance (Inset: Twist angle), **(b)** Radial distribution function (black) and running coordination number (red) between oxygen of amide group and chlorine atom of the chloroform. Color Scheme: Green-Carbon, Red-Oxygen, Blue-Nitrogen, Tan-Hydrogen and Magenta-Chlorine.

coordination number depicted in Fig. S7(b)), which once again demonstrates the stabilization of the stack by the solvent.

The diffusion coefficient is calculated from the Einstein equation via the mean square displacement (MSD). Plots of MSD from each simulation are shown in Fig. S8. The value reported in the main manuscript is the mean of the self diffusion coefficient obtained from these three runs.
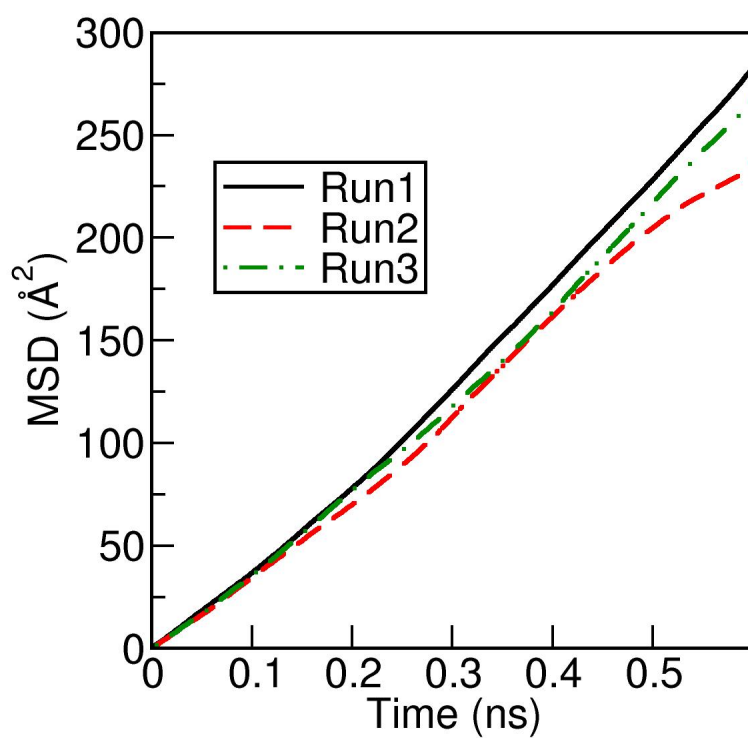
Figure S8: Mean squared displacment of [2.2]pCpTA-hex molecule in chloroform obtained from three independent simulations.

Oligomerization free energy simulations were carried out by considering six windows to scan the entire ξ as shown in Table S7, each one sampled for 25 ns using the ABF method. The reaction coordinate for the case of a dimer is depicted in Fig. S9(a) and (b). The free-energy difference are tabulated in Table. S11 To estimate the error in the free-energy difference, we performed three independent simulations in each window for a few oligomers for both [2.2]pCpTA-hex and BTA-hex. The error is calculated as the standard error of the mean and are shown in Fig. 3 of the main manuscript.
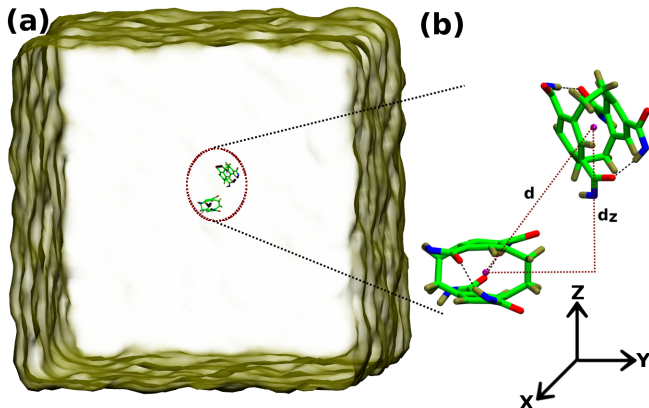

Figure S9: Free energy calculations: **(a)** Snapshot from MD simulations of dimer in chloroform, **(b)** Zoomed in portion of [2.2]pCpTA-hex dimer, the alkyl tails are not shown for clarity, "d" represents the distance between the center of mass of the two molecules, d_Z is the distance component along the stacking direction (z-direction). The color scheme is as described in Figure S6; in addition, magenta represents the pseduoatom to refer to the center of mass of the core in the [2.2]pCpTA-hex molecule.

**Table S11: Calculated free-energy difference ΔF_N using the ABF method.[a]**

| Size of the oligomer (N)	[2.2]pCpTA-hex (kcal/mol)	BTA-hex (kcal/mol)
2	-13.13	-13.30
3	-13.75	-15.50
4	-12.36	-14.95
5	-13.66	-15.52
6	-12.99	-16.64
7	-12.49	-15.87
8	-11.87	-16.07
9	-12.75	-15.28
10	-13.10	-16.60
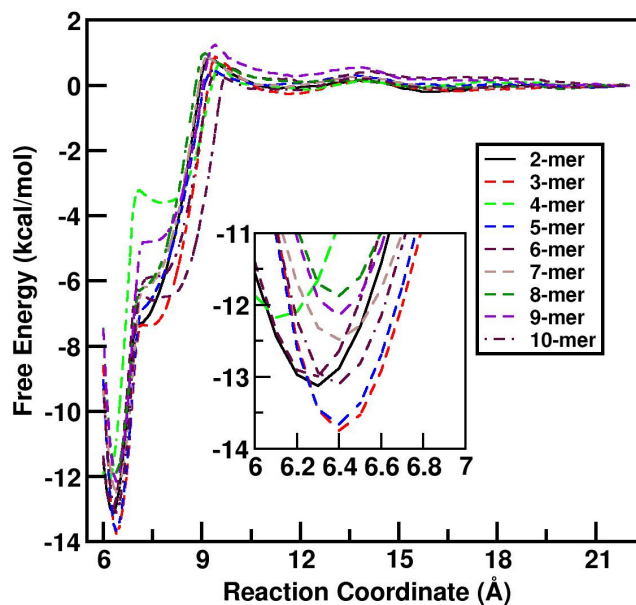
Figure S10: Free energy profile of [2.2]pCpTA-hex oligomers solvated in chloroform. The projection of distance between the top molecule in the oligomer and the dissociating monomer along the stacking direction is the collective variable. Inset shows the same data, near the free-energy minimum.
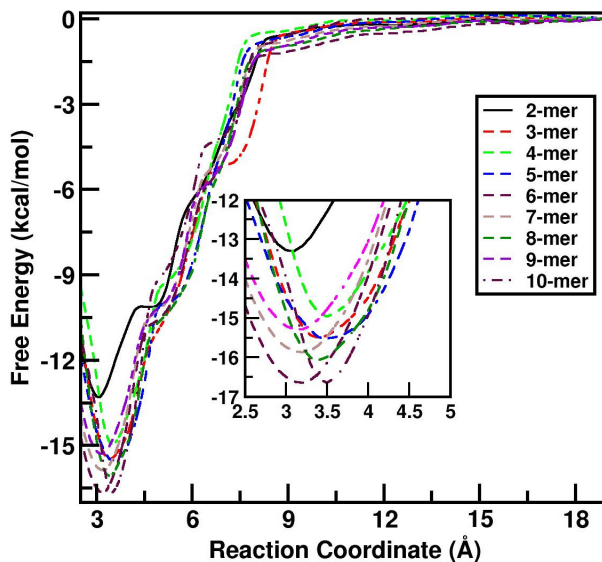
Figure S11: Free energy profile of BTA-hex oligomers solvated in *n*-nonane. The projection of distance between the top molecule in the oligomer and the dissociating monomer along the stacking direction is the collective variable. Inset shows the same data, near the free-energy minimum.
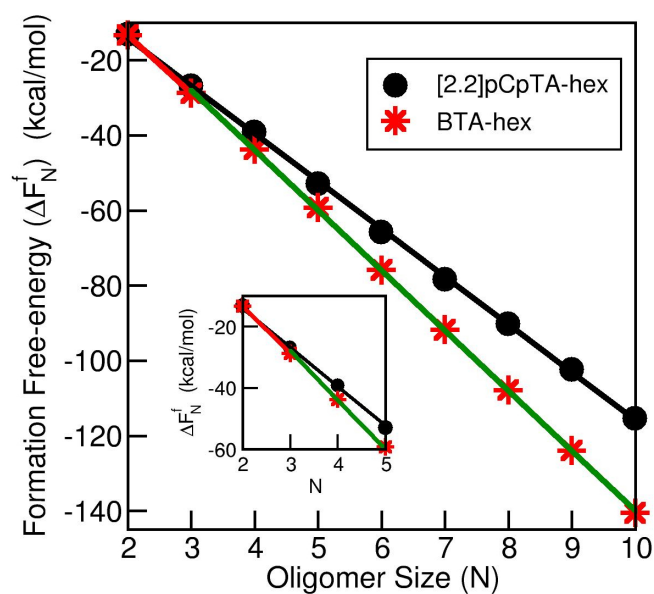
Figure S12: Free-energy of formation. The solid line represents a linear fit for the raw data shown as points.
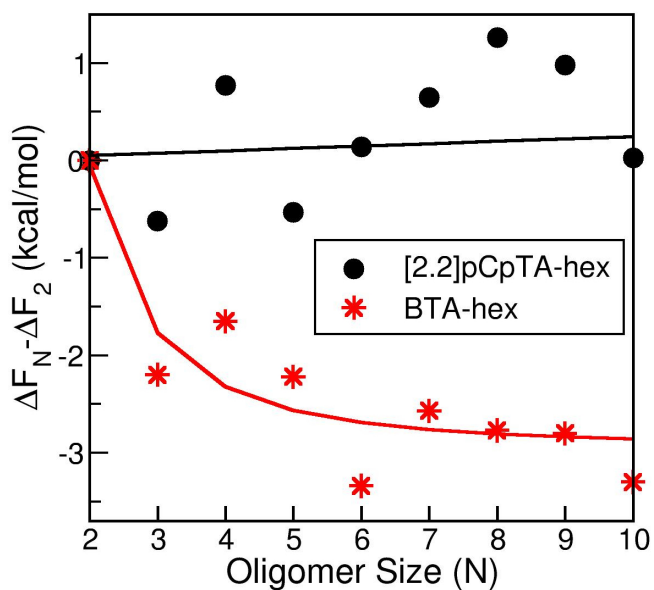

Figure S13: Deviations in free-energy difference from the dimerization free energy. The solid line is a guide to the eye.

The evolution of the dihedral angles over the WTM trajectory are shown in Fig S14(**b**) which indicates good sampling of the collective variables. The contour plot of dihedral angles is shown Fig. S14(**c**). The estimated barrier height for the anti to syn conversion is 10.2 kcal/mol and the free-energy difference ($\Delta F_{AS} = F_{anti} - F_{syn}$) between the conformations is 0.6 ± 0.2 kcal/mol, favoring the anti conformer. The results of a convergence test are shown in Fig. S14(**d**). The error is calculated from the block-analysis shown in Fig. S15. The high barrier in the FES prevents the molecule to explore the syn conformation in a normal MD simulation, although the free energy difference between the conformers is low.
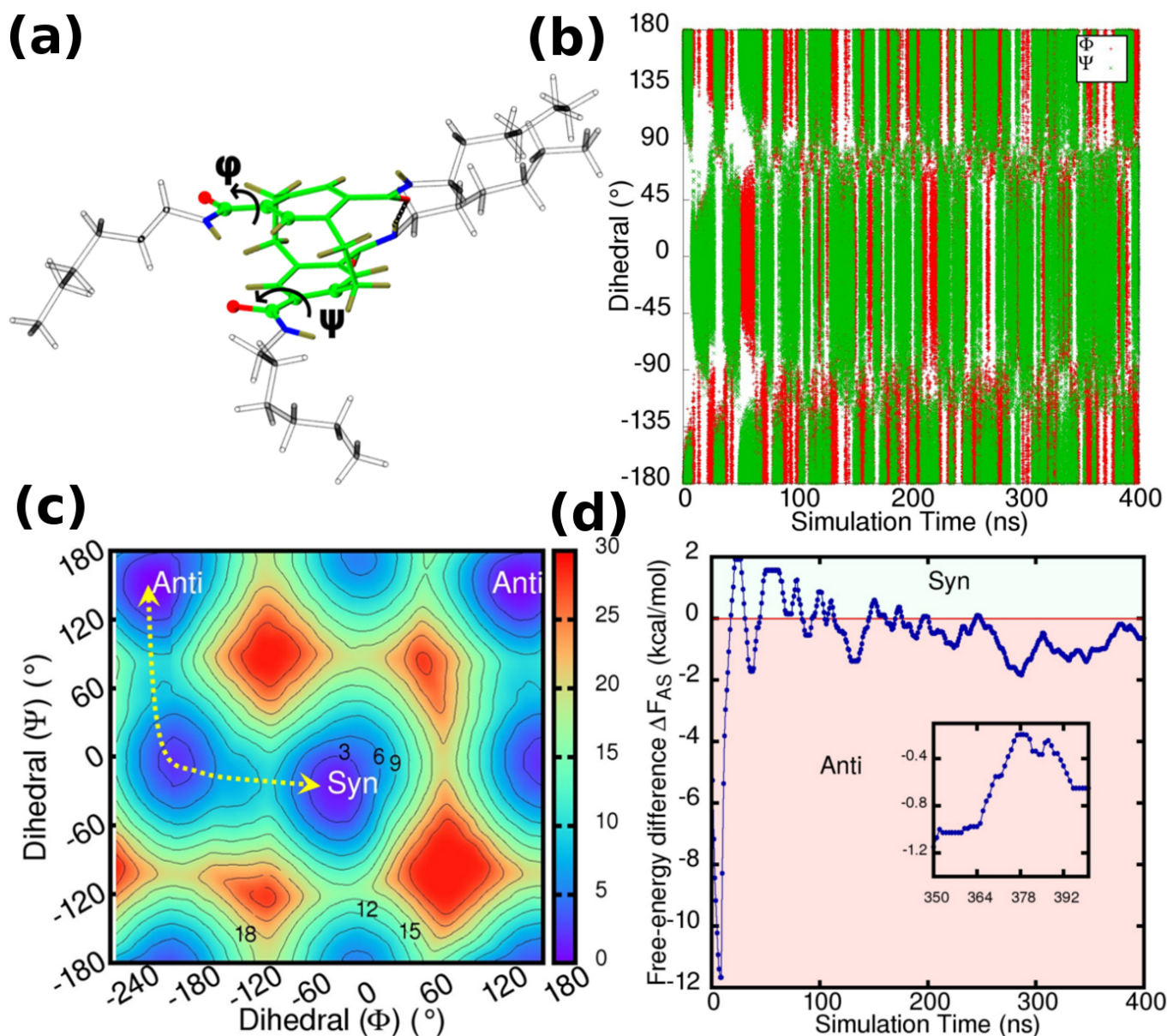
Figure S14: (a). Definition of the dihedrals Φ and Ψ in [2.2]pCpTA-hex molecule, as used in the well-tempered metadynamics simulations. The atoms which form the dihedral are shown in CPK representation. The color scheme is same as in Fig. S9 **(b)**. The time evolution of the dihedrals **(c)**. Contour maps of free-energy (kcal/mol) for dihedrals Φ and Ψ. The yellow dotted line serves as a guide to the eye showing the minimum free energy path followed by the [2.2]pCpTA-hex molecule to convert from its anti to syn conformation. **(d)**. Time evolution of free-energy difference (ΔF_{AS}). Anti and syn regions are labeled for clarity.

24
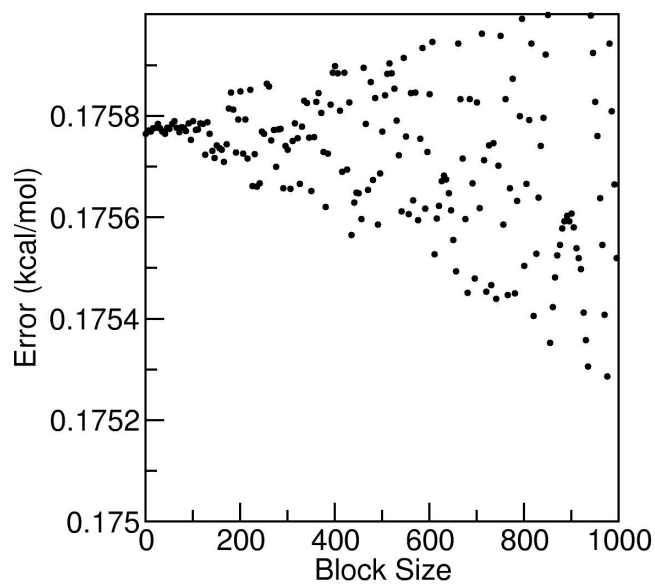
Figure S15: The error in free-energy calculations: Block analysis of a biased potential from well-tempered metadynamics simulation using Φ and Ψ as collective variables.

References

(1) Hutter, J.; Iannuzzi, M.; Schiffmann, F.; VandeVondele, J. CP2K: Atomistic Simulations of Condensed Matter Systems. *WIREs Comput Mol Sci* **2014**, *4*, 15–25.

(2) Perdew, J. P.; Burke, K.; Ernzerhof, M. Generalized Gradient Approximation Made Simple. *Phys. Rev. Lett.* **1996**, *77*, 3865.

(3) Goedecker, S.; Teter, M.; Hutter, J. Separable Dual-Space Gaussian Pseudopotentials. *Phys. Rev. B* **1996**, *54*, 1703.

(4) Grimme, S.; Antony, J.; Ehrlich, S.; Krieg, H. A Consistent and Accurate ab initio Parametrization of Density Functional Dispersion Correction (DFT-D) for the 94 Elements H-Pu. *J. Chem. Phys.* **2010**, *132*, 154104.

(5) Manz, T. A.; Sholl, D. S. Chemically Meaningful Atomic Charges that Reproduce the Electrostatic Potential in Periodic and Nonperiodic Materials. *J. Chem. Theory Comput.* **2010**, *6*, 2455–2468.

(6) Manz, T. A.; Sholl, D. S. Improved Atoms-in-molecule Charge Partitioning Functional for Simultaneously Reproducing the Electrostatic Potential and Chemical States in Periodic and Nonperiodic Materials. *J. Chem. Theory Comput.* **2012**, *8*, 2844–2867.

(7) Mayo, S. L.; Olafson, B. D.; Goddard, W. A. DREIDING: A Generic Force Field for Molecular Simulations. *J. Phys. Chem.* **1990**, *94*, 8897–8909.

(8) Fagnani, D. E.; Meese, M. J., Jr.; Abboud, K. A.; Castellano, R. K. Homochiral [2.2] Paracyclophane Self-Assembly Promoted by Transannular Hydrogen Bonding. *Angew. Chem. Int. Ed.* **2016**, *55*, 10726–10731.

(9) Plimpton, S. Fast parallel algorithms for short-range molecular dynamics. *J. Comput. Phys* **1995**, *117*, 1–19.

(10) Nosé, S. A unified formulation of the constant temperature molecular dynamics methods. *J. Chem. Phys.* **1984**, *81*, 511–519.

(11) Evans, D. J.; Holian, B. L. The nose–hoover thermostat. *J. Chem. Phys.* **1985**, *83*, 4069–4074.

(12) Swope, W. C.; Andersen, H. C.; Berens, P. H.; Wilson, K. R. A computer simulation method for the calculation of equilibrium constants for the formation of physical clusters of molecules: Application to small water clusters. *J. Chem. Phys.* **1982**, *76*, 637–649.

(13) Darve, E.; Rodríguez-Gómez, D.; Pohorille, A. Adaptive biasing force method for scalar and vector free energy calculations. *J. Chem. Phys.* **2008**, *128*, 144120.

(14) Fiorin, G.; Klein, M.; Hénin, J. Using collective variables to drive molecular dynamics simulations. *Mol. Phys.* **2013**, doi: 10.1080/00268976.2013.813594.

(15) Bejagam, K. K.; Balasubramanian, S. Supramolecular polymerization: a coarse grained molecular dynamics study. *J. Phys. Chem. B* **2015**, *119*, 5738–5746.

(16) Bejagam, K. K.; Fiorin, G.; Klein, M. L.; Balasubramanian, S. Supramolecular polymerization of benzene-1, 3, 5-tricarboxamide: a molecular dynamics simulation study. *J. Phys. Chem. B* **2014**, *118*, 5218–5228.

(17) Barducci, A.; Bussi, G.; Parrinello, M. Well-tempered metadynamics: a smoothly converging and tunable free-energy method. *Phys. Rev. Lett.* **2008**, *100*, 020603.

(18) Tribello, G. A.; Bonomi, M.; Branduardi, D.; Camilloni, C.; Bussi, G. PLUMED 2: New feathers for an old bird. *Comput. Phys. Commun.* **2014**, *185*, 604–613.

(19) Urbanaviciute, I.; Meng, X.; Cornelissen, T. D.; Gorbunov, A. V.; Bhattacharjee, S.; Sijbesma, R. P.; Kemerink, M. Tuning the Ferroelectric Properties of Trialkylbenzene-1, 3, 5-tricarboxamide (BTA). *Adv. Electron. Mater.* **2017**, *3*, 1600530.

(20) The Binding energy of an oligomer of size (N) is defined as, $B.E_N = \frac{E_N - N \cdot E_1}{(N-1)}$.

(21) DP_N, the scaled dipole moment, is the ratio of the electric dipole moment of a N-mer to the largest value of dipole moment observed in our calculations.

(22) Gilday, L. C.; Robinson, S. W.; Barendt, T. A.; Langton, M. J.; Mullaney, B. R.; Beer, P. D. Halogen bonding in supramolecular chemistry. *Chem. Rev.* **2015**, *115*, 7118–7195.

(23) Metrangolo, P.; Meyer, F.; Pilati, T.; Resnati, G.; Terraneo, G. Halogen bonding in supramolecular chemistry. *Angew. Chem. Int. Ed.* **2008**, *47*, 6114–6127.

(24) Xu, K.; Ho, D. M.; Pascal Jr, R. A. Azaaromatic chlorides: a prescription for crystal structures with extensive nitrogen-chlorine donor-acceptor interactions. *J. Am. Chem. Soc.* **1994**, *116*, 105–110.

(25) Müller, M.; Albrecht, M.; Gossen, V.; Peters, T.; Hoffmann, A.; Raabe, G.; Valkonen, A.; Rissanen, K. Anion–π Interactions in Salts with Polyhalide Anions: Trapping of I42-. *Chem.–Eur. J.* **2010**, *16*, 12446–12453.